

Published in final edited form as:

Invest Ophthalmol Vis Sci. 2008 September ; 49(9): 4145–4153. doi:10.1167/iov.07-1380.

Reprogramming Progeny Cells of Embryonic RPE to Produce Photoreceptors: Development of Advanced Photoreceptor Traits under the Induction of *neuroD*

Lina Liang¹, Run-Tao Yan¹, Xiumei Li^{1,2}, Melissa Chimento¹, and Shu-Zhen Wang¹

¹ Department of Ophthalmology, University of Alabama at Birmingham, Birmingham, Alabama

² Zhongshan Ophthalmic Center, Sun Yat-sen University, Guangzhou, China

Abstract

PURPOSE—In examining the prospect of producing functional photoreceptors by reprogramming the differentiation of RPE progeny cells, this study was conducted to investigate whether reprogrammed cells can develop highly specialized ultrastructural and physiological traits that characterize retinal photoreceptors.

METHODS—Cultured chick RPE cells were reprogrammed to differentiate along the photoreceptor pathway by ectopic expression of *neuroD*. Cellular ultrastructure was examined with electron microscopy. Cellular physiology was studied by monitoring cellular free calcium (Ca^{2+}) levels in dark-adapted cells in response to light and in light-bleached cells in response to 9-*cis*-retinal.

RESULTS—Reprogrammed cells were found to localize red opsin protein appropriately to the apex. These cells developed inner segments rich in mitochondria, and while in culture, some formed rudimentary outer segments, analogous to those of developing photoreceptors in the retina. In response to light, reprogrammed cells reduced their Ca^{2+} levels, as observed with developing retinal photoreceptors in culture. Further, on exposure to 9-*cis*-retinal, the light-bleached, reprogrammed cells increased their Ca^{2+} levels, reminiscent of visual cycle recovery.

CONCLUSIONS—These results indicate the potential of reprogrammed cells to develop advanced ultrastructural and physiological traits of photoreceptors and point to reprogramming progeny cells of embryonic RPE as a possible alternative in producing developing photoreceptors.

Photoreceptors are specialized sensory neurons in the retina. Their degeneration is a common cause of blindness from light damage, genetic changes, and aging.^{1,2} Because they are terminally differentiated and do not reenter the cell cycle for regeneration, photoreceptors that are lost cannot be replenished. The importance of photoreceptors to vision has spurred a spectrum of investigations ranging from photoreceptor rescue by trophic factors,³ supporting cells,^{4,5} or stem cells⁶ to photoreceptor replacement through retinal regeneration^{7–9} and transplantation.^{10,11} The recent demonstration of successful photoreceptor transplantation in blind mice¹² offers hope for vision rescue or restoration through cell replacement. It also heightens the importance of finding a source of photoreceptors, especially developing photoreceptors.¹³ One approach is to induce photoreceptor genesis through programming or reprogramming the differentiation of cells that can be propagated in large amounts. In recent years, brain, retinal, bone marrow, and embryonic stem cells have been explored in attempts to produce photoreceptors.^{14–20} Although these stem cells continue to be at center stage, there

Corresponding author: Shu-Zhen Wang, DB104, CEFH, 700 South 18th Street, Birmingham, AL 35294-0009; szwang@uab.edu.

Disclosure: L. Liang, None; R.-T. Yan, None; X. Li, None; M. Chimento, None; S.-Z. Wang, None

appears to be a need for alternative, perhaps provocative, sources of developing photoreceptors for cell-replacement studies.²¹

Unlike retinal neurons, the retinal pigment epithelial (RPE) cells from many species, including human, can reenter the cell cycle. More important, their progenies are able to differentiate into cell types other than RPE,²² raising a question of whether the RPE could be a source of retinal stem cells.²³ Making use of RPE cells' plasticity, we explored the possibility of using a regulatory gene to coax cultured RPE cells into differentiating along the photoreceptor pathway. *NeuroD*, which encodes a transcriptional factor belonging to the basic helix-loop-helix family, was tested, because of its instrumental role in photoreceptor differentiation and survival.²⁴⁻²⁷ Ectopic expression of *neuroD* in RPE cell cultures derived from day-6 chick embryos (E6) leads to de novo appearance of cells expressing photoreceptor-specific genes, including visinin, IRBP, α -PDE, opsins, and RaxL,^{24,25,28} a homeodomain gene essential for initiating photoreceptor differentiation.²⁹ When grafted into the subretinal space of embryonic chick eyes, those photoreceptor-like cells migrate into the photoreceptor layer of the retina and emanate axonal arborization into the outer plexiform layer.³⁰ Critical to the prospective functionality of such reprogrammed cells is their ability to develop structural features and functional properties characteristic of highly specialized photoreceptors. We report that reprogrammed cells developed ultrastructural features typical of developing photoreceptors. They responded to light by decreasing their cellular free-calcium (Ca^{2+}) levels. On exposure of light-bleached cells to 9-*cis*-retinal, their Ca^{2+} levels were elevated, a reaction reminiscent of the Ca^{2+} increase on visual cycle recovery. These results provide support to the prospect of guiding RPE progeny cells to differentiate into photoreceptors.

MATERIALS AND METHODS

Chick Embryos

Fertilized, pathogen-free White Leghorn chicken eggs were purchased from Spafas (Norwich, CT) and incubated (Petersime, Gettysburg, OH). All use of animals adhered to the ARVO Statement for the Use of Animals in Ophthalmic and Vision Research and to the procedures and policies set by the institutional review board at the University of Alabama at Birmingham.

Cell Culture

Chick E6 RPE was isolated as previously described.²⁴ RPE cells were dissociated with trypsin/EDTA and cultured with knockout DMEM supplemented with 20% serum replacement (Invitrogen, Carlsbad, CA) in 35-mm culture dishes. When the cells reached approximately 50% confluence, 20 μL of concentrated RCAS-neuroD retrovirus, or RCAS-GFP as a negative control, was added to each culture dish. The viral stocks were prepared as previously described,²⁴ and their titers ranged from 0.7 to 3×10^8 pfu/mL. The cultures were maintained for an additional 8 to 10 days with medium 199 (M199) supplemented with 10% fetal calf serum, before the cells were fixed for immunostaining and EM preparation or the live cells were subjected to Ca^{2+} imaging.

To obtain isolated cells, cells from a primary culture infected with RCAS-neuroD were trypsinized, reseeded onto polyornithine-treated coverslips at ~1–3 dilution, and cultured for 3 to 6 days with M199 plus 10% fetal calf serum.

E16 and E19 retinas were isolated. The retinal cells were dissociated with trypsin/EDTA, seeded onto polyornithine-treated substratum, cultured for 3 to 8 days with M199 plus 10% fetal calf serum.

Immunocytochemistry

Monoclonal antibody against visinin (7G4, 1:500; developed by Constance Cepko; Department of Genetics, Harvard Medical School, Howard Hughes Medical Institute, Boston, MA) was obtained from the Developmental Studies Hybridoma Bank (University of Iowa). Polyclonal antibodies against red opsin (1:200) were purchased from Chemicon (Temecula, CA). Standard immunocytochemistry was performed with alkaline phosphatase- or horseradish peroxidase-conjugated secondary antibodies (Vector Laboratories, Burlingame, CA), as described by the manufacturers. For double-labeling, anti-visinin was recognized with horseradish peroxidase-conjugated secondary antibody, and anti-red opsin was recognized with alkaline phosphatase-conjugated secondary antibody.

In Situ Hybridization

Sequences corresponding the cone type α -subunit of transducin (GenBank accession number NM_204690; <http://www.ncbi.nlm.nih.gov/Genbank>; provided in the public domain by the National Center for Biotechnology Information, Bethesda, MD), the α -subunit of cone cGMP-gated channel (*CNGA3*; GenBank accession number NM_205221), and the α -subunit of rod cGMP-gated channel (*CNGA1*; GenBank accession number NM_205220) were PCR amplified from chick retinal cDNA. PCR products were cloned into pGEM-T, and their sequences were subsequently verified. Linearized plasmids harboring the sequences were used to synthesize digoxigenin (DIG)-labeled antisense RNA probes (Genius kit; Roche Molecular Biochemicals, Indianapolis, IN) according to the manufacturer's instructions. In situ hybridization was performed as previously described.²⁵

Calcium Imaging of Light Response

Cells in a 35-mm culture dish were rinsed twice with M199 and incubated at 37°C for 30 minutes with 2 mL of M199 containing 4 μ M Fluo-4 AM (Invitrogen-Molecular Probes, Eugene, OR) prepared as described by Li et al.³¹ The culture dish was rinsed twice, both before and after incubation with M199 for 15 minutes at 37°C. The dish with 2 mL of M199 was placed on the stage of an inverted microscope (model TE300; Nikon, Tokyo, Japan) equipped with a 100 W-HBO mercury light source and a 40 \times objective for fluorescent photomicrography. Images were captured with a digital camera (2-second exposure; MicroPublisher 5.0; Q-Imaging, Surrey, BC, Canada) using a filter set with maximum excitation of 488 nm and emission at 517 nm. After the initial image was captured, cells in the dish were subjected to visible light (set at the maximum) on the microscope for various lengths of time. Immediately after the light exposure, another fluorescent image was captured (2-second exposure). All steps were performed with room lights off.

For postimaging molecular identification, cells were fixed with 4% paraformaldehyde after Ca²⁺ imaging and subjected to immunostaining with anti-visinin antibody. For experiments with cyclic nucleotide gated (CNG) channel blockers, reprogrammed cultures were processed as described in the previous paragraph up to the final wash with M199. At this point, 2 mL of M199 containing 3 μ M each of dichlorobenzamil and L-*cis*-diltiazem was added, and the culture dish was then placed on the microscope for imaging. Dichlorobenzamil and L-*cis*-diltiazem were purchased from Sigma-Aldrich (St. Louis, MO) and dissolved into DMSO (30 mM stock solution).

The integrated optical density (IOD) of a cell was measured with commercial image-analysis software (LabWorks, ver. 4.0, UVP Inc., Upland, CA). The means and SDs of IODs from three to nine cells were calculated (Origin 7.0; OriginLab Corp. Northampton, MA).

Calcium Imaging of Response to 9-*cis*-Retinal

Cells in a primary RPE cell culture infected with RCAS-neuroD were trypsinized and reseeded at lower density (see Cell Culture). The reseeded culture was incubated with 4 μ M Fluo-4 AM, as described in the previous section. After the cells were subjected to visible light (set at the maximum) on the microscope stage for 1 to 3 minutes, either 50 μ L of vehicle control (DMSO, 1:100 dilution with M199) or 50 μ L of 0.5 mM 9-*cis*-retinal was applied with a pipette aimed directly above the viewing area without disturbing the 35-mm dish containing 2 mL of M199. Images were captured at different time points. 9-*cis*-Retinal was purchased from Sigma-Aldrich and dissolved in DMSO for a 50 mM stock solution. Before use, the stock solution was diluted 1:100 with M199. For experiments with the same cells subjected to both vehicle control and 9-*cis*-retinal, 50 μ L of vehicle control was applied, and images were captured at various time points. Medium in the dish was replaced, and 50 μ L of 0.5 mM 9-*cis*-retinal was applied. All steps were performed with room lights off.

Electron Microscopy

An E17 chick eye was placed in a fixative solution consisting of 2.5% glutaraldehyde and 2% paraformaldehyde in 0.1 M phosphate buffer. With the eye immersed in fixative, a small piece of the central retina was isolated, and fixation was continued for 3 hours. After three washes, the retinal sample was postfixed with osmium tetroxide, stained with uranyl acetate, dehydrated through a series of graded ethanol and 100% propylene oxide, infiltrated with a 1:1 mixture of 100% propylene oxide and epoxy resin (Polybed 812; PolySciences, Warrenton, PA), and embedded and polymerized in 100% resin. Ultrathin sections (70–90 nm thick) were examined with a transmission electron microscope (1200 EX II; JEOL, Tokyo, Japan).

For RPE cell cultures, the cell layer in a 35-mm culture dish was carefully peeled off and subjected to the same fixation procedure as was used for the retinal tissue, except that the propylene oxide was replaced with ethanol.

RESULTS

Subcellular Localization of Red Opsin

RPE cells lose their pigmentation when they proliferate in culture and become repigmented as the culture becomes confluent.³⁰ Essentially all cells in the culture can be infected with RCAS as a result of primary and subsequent infections by this replication-competent retrovirus.²⁴ In RPE cultures infected with RCAS-neuroD, a large number of cells (but usually <30% the total³⁰) expressed visinin (Fig. 1A). Visinin is a calcium-binding protein and an early marker for chick cones.³² No visinin⁺ cells were detected in the control culture infected with RCAS-GFP (Fig. 1B). In previous studies, in situ hybridization, RT-PCR, and immunochemical analyses have shown that transdifferentiating cells express an array of additional photoreceptor-specific genes, including *IRBP*, *aPDE*, opsins (red, green, blue, and rhodopsin), and *RaxL*.^{24,25,28} Cells expressing photoreceptor-specific genes appeared to be the major, if not the only, product in *neuroD*-induced transdifferentiation.²⁴ To examine whether opsin protein was synthesized and appropriately localized, we used a specific antibody against red opsin, the most abundant among all opsins in the cone-dominant chick retina. The antibody identified many positive cells (estimated to account for approximately 70% of visinin⁺ cells based on double-staining experiments) in RPE cell cultures infected with RCAS-neuroD (Fig. 1C), but not in control cultures infected with RCAS-GFP (data not shown). The red opsin⁺ cells were of two types, one with punctate, dotlike staining, and the other in clusters with their cytoplasmic compartments showing immunostaining (Fig. 1C). The dotlike staining was more pronounced in areas where more pigmented RPE cells were present in the culture and was observed in 10% to 20% of total cells present in the area. At higher magnification, the “dots,” when present, appeared to decorate the cellular apices (Fig. 1D). This was further shown by

double immunostaining. Red opsin immunostaining was detected at the apices of visinin⁺ cells (Fig. 1E). Thus, in primary culture at places with significant RPE repigmentation, reprogrammed cells correctly localized red opsin protein.

In reseeded culture, most of the anti-red opsin immunoreactivity was detected at the inner segment compartment (Fig. 1F). Similar mislocalization was observed with retinal photoreceptor cells in culture (Fig. 1G). Opsin mislocalization occurs when photoreceptors are separated from RPE.^{33–35}

Ultrastructural Features

Structural hallmarks of photoreceptors are the inner segment and the outer segment. The single most important feature of the inner segment is the presence of a large number of mitochondria to accommodate high-energy demand. The outer segment is characterized by the presence of stacks of membranous discs to house the biochemical components necessary for converting light into electrophysical signals and initiating the phototransduction pathway.³⁶ From E15 to hatching, chick photoreceptor cells undergo rapid structural differentiation. The outer segments of the rods and cones appear on E15.³⁷ Transmission electron microscopy showed that reprogrammed cells displayed cellular compartments characteristic of inner segments densely populated with mitochondria (Figs. 2D–F) and closely resembling the inner segments of photoreceptor cells in E17 chick retina (Fig. 2H). These mitochondria-rich regions were not observed in the control RPE cells, which typically contained pigment granules (Figs. 2A–C). Based on the frequency at which a mitochondria-rich region was observed among the specimens examined, we estimated that inner segments were present in approximately 80% of the reprogrammed cells that were visinin⁺. On the apex of the inner segment, reprogrammed cells displayed ciliary expansions (Fig. 2D, arrowhead), reminiscent of the developing outer segments of photoreceptors in E17 retina (Fig. 2H) or in culture as described.³⁸ These ciliary expansions contained membranous, disclike structures (Figs. 2E–G) that were similar to the developing outer segments of retinal photoreceptors in ovo (Figs. 2I–J). These membranous, disclike structures were irregularly arranged. Occasionally, reprogrammed cells developed discernible discs (Fig. 2G, white arrow), similar to those of developing photoreceptor cells (Fig. 2J, 2K).

Additional structural features of photoreceptors were observed in reprogrammed cells. These included the lipid droplet (Fig. 2F, asterisk), typical of chick photoreceptors (Figs. 2H, 2I), and the calyx (Fig. 2G, white arrowhead), a cuplike extension of plasma membrane from the apex of the inner segment along the basal region of the outer segment, as in retinal photoreceptors (Fig. 2I).

Reduction in Ca²⁺ Levels in Response to Light

Photoreceptors in the dark are depolarized, and their intra-cellular Ca²⁺ levels are high. Light hyperpolarizes the cells and causes a decrease in their Ca²⁺ level because of the ion-exchangers continue to extrude calcium after the light-driven closure of cGMP-gated channels.^{39,40} To address whether reprogrammed cells would develop this physiological trait, we examined their Ca²⁺ levels in response to light, using the Ca²⁺ indicator Fluo-4 AM. As a reference, E16 retinal cells were dissociated and cultured for 3 days (equivalent to E19, when the chick retina becomes capable of visual function⁴¹), and their Ca²⁺ levels were similarly monitored. In the control RPE cell culture infected with RCAS, the cells were basically invisible (i.e., their Ca²⁺ level was below the detection limit) and remained so throughout the experiment (Fig. 3A). In RPE cell cultures infected with RCAS-neuroD, the Ca²⁺ indicator identified a large number of cells that were morphologically neuronlike (Figs. 3B–D), whereas the remaining, probably nonreprogrammed, RPE cells were invisible. On light stimulation, some of the reprogrammed cells exhibited a detectable reduction in their Ca²⁺ levels. Computer-assisted calculation of

IOD showed ~60% reduction in their fluorescent intensities. Most of the reduction appeared to have occurred during the first 0.5 minute of light exposure (Fig. 3B). Extending the light exposure to 1 minute gave only a modest additional reduction (Fig. 3B). Similarly, continuing the light exposure after the first minute for an additional 1 minute (Fig. 3C) or 3 minutes (Fig. 3D) did not produce major additional reductions. These indicated that the observed reduction in fluorescent intensities were not due to slow Ca^{2+} leakage from these cells over time.

The levels of reduction differed among reprogrammed cells, with some showing reductions readily discernible to the human eye (Figs. 3C, 3D, arrows), whereas some seemed to lack obvious reductions regardless of the length of light exposure (Figs. 3C, 3D, arrowheads). IOD measurements confirmed the variation. The difference in light responsiveness was expected, since reprogrammed cells were not uniform in their levels of differentiation.

In retinal cell culture, photoreceptor cells, marked by the lipid droplet (Figs. 3E, black arrowhead), also showed a reduction in Ca^{2+} levels after exposure to light. A 10-second (0.17-minute) light exposure produced a moderate effect, ~12% reduction in IOD. A further 1-minute exposure yielded a more pronounced effect, a total of ~60% reduction in IOD (Fig. 3E). Overall, the Ca^{2+} reductions of cultured photoreceptor cells appeared similar to that of reprogrammed cells with conspicuous photoreceptor-like morphologies.

Post- Ca^{2+} -imaging immunostaining was used to confirm the photoreceptor identify of cells showing light responses. Immunostaining with antibodies against visinin, a protein equivalent of the mammalian recoverin,⁴² identified cells that had exhibited Ca^{2+} reduction after light exposure (Figs. 4A–D). To test whether reprogrammed cells expressed additional phototransduction components, besides visinin, α -PDE, and opsin genes (red, green, blue, and rhodopsin),²⁵ we examined the expression of cone α -transducin and the α -subunits of cone (A3) and rod (A1) CNG channels.⁴³ In situ hybridization detected cells expressing cone α -transducin and CNGA1/A3 in reprogrammed cultures (Figs. 4F, 4H), but not in the control cultures (Figs. 4E, 4G). Because the in situ hybridization procedure itself adversely results in poor preservation of cellular morphologies (compared with immunostaining), it is difficult to gauge the true morphologies of cells expressing the phototransduction genes. Nevertheless, these cells appeared photoreceptor-like, with a compact cell body and an inner-segment-like compartment stained by in situ hybridization.

CNG channels mediate vertebrate photoreceptor phototransduction and can be inhibited by dichlorobenzamil⁴⁴ and L-*cis*-diltiazem.⁴⁵ To address the question of whether the reduction in Ca^{2+} after exposure to light in reprogrammed cells was a response to light, we examined Ca^{2+} levels before and after a light exposure in the presence of these two CNG channel blockers. We found no reduction in Ca^{2+} levels among reprogrammed cells after exposure to light for 1 minute and 2 minutes; even in cells with discernible photoreceptor morphologies, the Ca^{2+} levels did not decrease after exposure to light (Fig. 5).

Ca^{2+} Increase in Response to 9-*cis*-Retinal

Another hallmark of photoreceptor physiology is the functional recovery of visual pigments when light-bleached photoreceptors are provided with the chromophore 11-*cis*-retinal or its analogue, 9-*cis*-retinal.⁴⁶ One of the many outcome measures of visual recovery is an increase in Ca^{2+} levels.⁴⁷ To test whether the reprogrammed cells developed this property, we monitored the Ca^{2+} levels of light-bleached cells before and after the administration of 9-*cis*-retinal and compared the response with those of developing photoreceptor cells. Cells from an RPE cell culture infected with RCAS-neuroD were reseeded at low density to minimize potential input from nonreprogrammed RPE cells. Ca^{2+} levels of light-bleached, photoreceptor-like cells were found to increase several fold within a few minutes after the addition of 9-*cis*-retinal (Fig. 6A). No changes were observed with the vehicle (DMSO) control.

To demonstrate this further, we subjected the same cells first to DMSO and then to 9-*cis*-retinal. Although with DMSO Ca^{2+} levels remained basically the same throughout the imaging period of 10 minutes (Fig. 6B), approximately 3 minutes after the application of 9-*cis*-retinal, Ca^{2+} levels increased (Fig. 6B). Similar responses were observed with developing photoreceptor cells derived from E19 chick retina (Figs. 6C, 6D). Photoreceptor cells in the retinal cell culture were identified by their morphology and a lipid droplet (Figs. 6C, 6D, black arrowhead).

Increased Ca^{2+} levels were observed only with cells conspicuously displaying photoreceptor-like morphologies in the reprogrammed population (Figs. 6A, 6B; Figs. 7A, 7B, arrow) and in a retinal cell culture (Figs. 6C, 6D). These morphologic features included elongated cell bodies, an easily discernible inner segment (red arrowhead) with conspicuous lipid-droplet (black arrowhead), an apical expansion (green arrowhead), and a long process emanating from the basal side. Cells lacking such highly specialized morphologies in the reprogrammed culture (Figs. 7A, 7B, arrowhead) and in retinal cell culture (Fig. 6D, arrowhead) showed no changes in their Ca^{2+} levels. In the reprogrammed population, cells maintaining the morphologies of cultured RPE cells (Fig. 7A, asterisks) remained invisible, similar to those in the primary cultures (Fig. 6A). The increase in Ca^{2+} levels in response to 9-*cis*-retinal was also observed in cells showing physical contact with other cells (Fig. 7B).

DISCUSSION

For their unique function in capturing photons and initiating the visual cascade, photoreceptors develop discrete structural and functional traits. They form inner segments packed with mitochondria, and they grow outer segments that consist of stacks of membranous discs. In RPE cell cultures infected with RCAS-neuroD, reprogrammed cells displayed inner segments. Some showed rudimentary outer segments, including electron-dense discs. Compared to inner segments, outer-segment-like structures were observed at a reduced frequency. This redundancy could mainly be due to the *in vitro* conditions not being permissive for outer segment formation. Even retinal photoreceptor cells grown in culture can only develop irregularly arranged, membranous structures.⁴⁸ In addition, separating photoreceptors from the RPE prevents normal assembly of disc membranes.^{49,50} In light of these findings, we do not expect the reprogrammed cells to show well-formed outer segments under the experimental conditions.

Light hyperpolarizes photoreceptors and causes a decrease in cytosolic Ca^{2+} .⁵¹ This physiological property differs diametrically from that of intrinsically photosensitive retinal ganglion cells.^{52,53} Reprogrammed cells were found to reduce their Ca^{2+} on light stimulation, similar to developing photoreceptors. The levels of reduction varied among reprogrammed cells. The variation could be caused by varied levels of differentiation along the photoreceptor pathway. Gleason et al.⁵⁴ reported increases in Ca^{2+} on depolarization in chick photoreceptor cells close to maturity, but not in younger cells. Varied light responses have also been reported among developing frog photoreceptors.⁵⁵

Deep declines in Ca^{2+} levels occurred within the first half-minute after light exposure. This time frame of major Ca^{2+} reduction agrees with the Ca^{2+} extrusion mode of the photoreceptor calcium exchanger, which operates in a brief 10 to 30 seconds of high-velocity activity, followed by a nearly complete inactivation.⁵⁶ It is also consistent with the results by Gleason et al.⁵⁴ who observed that the levels of Ca^{2+} in cultured, developing chick cones declined within 30 seconds and stabilized at a new level within 70 seconds after potassium-induced depolarization. These agreements indicate similarities in light response between the reprogrammed cells and developing photoreceptor cells from the retina.

Subjecting light-bleached, reprogrammed cells to 9-*cis*-retinal increased their Ca²⁺ levels. The increases were comparable to those observed with light-bleached, cultured developing photoreceptor cells. This strengthens the support for physiological resemblance of the reprogrammed cells with developing photoreceptors.

Together, the similarities between reprogrammed cells and developing photoreceptor cells in ultrastructure, the subcellular localization of red opsin, the response to light, and the response to 9-*cis*-retinal indicate that *neuroD* induced advanced photoreceptor differentiation in the context of non-neural RPE progeny cells. The capability for highly specialized ultrastructural and physiological differentiation of the reprogrammed cells improves the prospect of exploring this system to produce functional photoreceptors.

Acknowledgements

The authors thank Stephen Hughes for retroviral vector RCAS, Marie Burns and Krzysztof Palczewski for suggestions on experiments involving 9-*cis*-retinal, and Christine Curcio for guidance on electron photomicrography and comments on the manuscript.

Supported by NIH/NEI Grants EY11640 (SZW) and EY06109 (CC, supporting MC) and Research to Prevent Blindness. LL is a Charles Kelman Postdoctoral Scholar of the International Retinal Research Foundation. XL received a scholarship from the Chinese Scholarship Council.

References

1. Papermaster DS, Windle J. Death at an early age: apoptosis in inherited retinal degenerations. *Invest Ophthalmol Vis Sci* 1995;36:977–983. [PubMed: 7730031]
2. Milam AH, Li ZY, Fariss RN. Histopathology of the human retina in retinitis pigmentosa. *Prog Retin Eye Res* 1998;17:175–205. [PubMed: 9695792]
3. Adler R, Curcio C, Hicks D, Price D, Wong F. Cell death in age-related macular degeneration. *Mol Vis* 1999;5:31. [PubMed: 10562655]
4. LaVail MM. Legacy of the RCS rat: impact of a seminal study on retinal cell biology and retinal degenerative diseases. *Prog Brain Res* 2001;131:617–627. [PubMed: 11420975]
5. Bennett J. Gene therapy for Leber congenital amaurosis. *Novartis Found Symp* 2004;255:195–202. [PubMed: 14750605]
6. Otani A, Dorrell MI, Kinder K, et al. Rescue of retinal degeneration by intravitreally injected adult bone marrow-derived lineage-negative hematopoietic stem cells. *J Clin Invest* 2004;114:765–774. [PubMed: 15372100]
7. Raymond PA. Retinal regeneration in teleost fish. *Ciba Found Symp* 1991;160:171–186. [PubMed: 1752162]
8. Stenkamp DL, Cameron DA. Cellular pattern formation in the retina: retinal regeneration as a model system. *Mol Vis* 2002;8:280–293. [PubMed: 12181523]
9. Otteson DC, Hitchcock PF. Stem cells in the teleost retina: persistent neurogenesis and injury-induced regeneration. *Vision Res* 2003;43:927–936. [PubMed: 12668062]
10. Aramant RB, Seiler MJ. Retinal transplantation: advantages of intact fetal sheets. *Prog Retin Eye Res* 2002;21:57–73. [PubMed: 11906811]
11. Young MJ. Stem cells in the mammalian eye: a tool for retinal repair. *APMIS* 2005;113:845–857. [PubMed: 16480454]
12. MacLaren RE, Pearson RA, MacNeil A, et al. Retinal repair by transplantation of photoreceptor precursors. *Nature* 2006;444:203–207. [PubMed: 17093405]
13. Bennett J. Retinal progenitor cells: timing is everything. *N Engl J Med* 2007;356:1577–1579. [PubMed: 17429090]
14. Takahashi M, Palmer TD, Takahashi J, Gage FH. Widespread integration and survival of adult-derived neural progenitor cells in the developing optic retina. *Mol Cell Neurosci* 1998;12:340–348. [PubMed: 9888988]

15. Young MJ, Ray J, Whiteley SJ, Klassen H, Gage FH. Neuronal differentiation and morphological integration of hippocampal progenitor cells transplanted to the retina of immature and mature dystrophic rats. *Mol Cell Neurosci* 2000;16:197–205. [PubMed: 10995547]
16. Nishida A, Takahashi M, Tanihara H, et al. Incorporation and differentiation of hippocampus-derived neural stem cells transplanted in injured adult rat retina. *Invest Ophthalmol Vis Sci* 2000;41:4268–4274. [PubMed: 11095625]
17. Kicic A, Shen WY, Wilson AS, Constable IJ, Robertson T, Rakoczy PE. Differentiation of marrow stromal cells into photoreceptors in the rat eye. *J Neurosci* 2003;23:7742–7749. [PubMed: 12944502]
18. Chen Y, Teng FY, Tang BL. Coaxing bone marrow stromal mesenchymal stem cells towards neuronal differentiation: progress and uncertainties. *Cell Mol Life Sci* 2006;63:1649–1657. [PubMed: 16786223]
19. Meyer JS, Katz ML, Maruniak JA, Kirk MD. Embryonic stem cell-derived neural progenitors incorporate into degenerating retina and enhance survival of host photoreceptors. *Stem Cells* 2006;24:274–283. [PubMed: 16123383]
20. Lamba DA, Karl MO, Ware CB, Reh TA. Efficient generation of retinal progenitor cells from human embryonic stem cells. *Proc Natl Acad Sci USA* 2006;103:12769–12774. [PubMed: 16908856]
21. Reh TA. Neurobiology: right timing for retina repair. *Nature* 2006;444:156–157. [PubMed: 17093406]
22. Zhao S, Rizzolo LJ, Barnstable CJ. Differentiation and transdifferentiation of the retina pigment epithelium. *Int Rev Cytol* 1997;171:225–265. [PubMed: 9066129]
23. Fischer AJ, Reh TA. Transdifferentiation of pigmented epithelial cells: a source of retinal stem cells? *Dev Neurosci* 2001;23(4–5):268–276. [PubMed: 11756742]
24. Yan R-T, Wang S-Z. neuroD induces photoreceptor cell overproduction in vivo and de novo generation in vitro. *J Neurobiol* 1998;36:485–496. [PubMed: 9740021]
25. Yan R-T, Wang S-Z. Expression of an array of photoreceptor genes in chick embryonic RPE cell cultures under the induction of neuroD. *Neurosci Lett* 2000;280:83–86. [PubMed: 10686383]
26. Yan R-T, Wang S-Z. Requirement of NeuroD for photoreceptor formation in the chick retina. *Invest Ophthalmol Vis Sci* 2004;45:48–58. [PubMed: 14691153]
27. Pennesi ME, Cho JH, Yang Z, et al. BETA2/NeuroD1 null mice: a new model for transcription factor-dependent photoreceptor degeneration. *J Neurosci* 2003;23:453–461. [PubMed: 12533605]
28. Ma W, Yan R-T, Xie W, Wang S-Z. bHLH genes *cath5* and *cNSCL1* promote bFGF-stimulated RPE cells to transdifferentiate towards retinal ganglion cells. *Dev Biol* 2004;265:320–328. [PubMed: 14732395]
29. Chen CM, Cepko CL. The chicken *RaxL* gene plays a role in the initiation of photoreceptor differentiation. *Development* 2002;129:5363–5375. [PubMed: 12403708]
30. Liang L, Ma W, Yan R-T, Zhang H, Wang S-Z. Exploring RPE as a source of photoreceptors: differentiation and integration of reprogrammed cells grafted into embryonic chick eyes. *Invest Ophthalmol Vis Sci* 2006;47:5066–5074. [PubMed: 17065528]
31. Li H, Ferrari MB, Kuenzel WJ. Light-induced reduction of cytoplasmic free calcium in neurons proposed to be encephalic photoreceptors in chick brain. *Brain Res Dev Brain Res* 2004;153:153–161.
32. Yamagata K, Goto K, Kuo CH, Kondo H, Miki N. Visinin: a novel calcium binding protein expressed in retinal cone cells. *Neuron* 1990;4:469–476. [PubMed: 2317380]
33. Bok D. The retinal pigment epithelium: a versatile partner in vision. *J Cell Sci* 1993;17(suppl):189–195.
34. Townes-Anderson E, St Jules RS, Sherry DM, Lichtenberger J, Hassanain M. Micromanipulation of retinal neurons by optical tweezers. *Mol Vis* 1998;4:12. [PubMed: 9701608]
35. Linberg KA, Sakai T, Lewis GP, Fisher SK. Experimental retinal detachment in the cone-dominant ground squirrel retina: morphology and basic immunocytochemistry. *Vis Neurosci* 2002;19:603–619. [PubMed: 12507327]
36. Burns ME, Arshavsky VY. Beyond counting photons: trials and trends in vertebrate visual transduction. *Neuron* 2005;48:387–401. [PubMed: 16269358]

37. Coulombre AJ. Correlations of structural and biochemical changes in the developing retina of the chick. *Am J Anat* 1955;96:153–189. [PubMed: 14361308]
38. Adler R, Lindsey JD, Elsner CL. Expression of cone-like properties by chick embryo neural retina cells in glial-free monolayer cultures. *J Cell Biol* 1984;99:1173–1178. [PubMed: 6470040]
39. Yau KW, Nakatani K. Light-induced reduction of cytoplasmic free calcium in retinal rod outer segment. *Nature* 1985;313:579–582. [PubMed: 2578628]
40. Sampath AP, Matthews HR, Cornwall MC, Bandarchi J, Fain GL. Light-dependent changes in outer segment free-Ca²⁺ concentration in salamander cone photoreceptors. *J Gen Physiol* 1999;113:267–277. [PubMed: 9925824]
41. Lindeman VF. The cholinesterase and acetylcholine content of the chick retina, with especial reference to functional activity as indicated by the pupillary constrictor reflex. *Am J Physiol* 1947;148:40–44.
42. Polans AS, Burton MD, Haley TL, Crabb JW, Palczewski K. Recoverin, but not visinin, is an autoantigen in the human retina identified with a cancer-associated retinopathy. *Invest Ophthalmol Vis Sci* 1993;34:81–90. [PubMed: 8425844]
43. Bonigk W, Altenhofen W, Muller F, et al. Rod and cone photoreceptor cells express distinct genes for cGMP-gated channels. *Neuron* 1993;10:865–877. [PubMed: 7684234]
44. Nicol GD, Schnetkamp PP, Saimi Y, Cragoe EJ Jr, Bownds MD. A derivative of amiloride blocks both the light-regulated and cyclic GMP-regulated conductances in rod photoreceptors. *J Gen Physiol* 1987;90:651–669. [PubMed: 2826642]
45. Haynes LW. Block of the cyclic GMP-gated channel of vertebrate rod and cone photoreceptors by 1-cis-diltiazem. *J Gen Physiol* 1992;100:783–801. [PubMed: 1282145]
46. Pepperberg DR, Brown PK, Lurie M, Dowling JE. Visual pigment and photoreceptor sensitivity in the isolated skate retina. *J Gen Physiol* 1978;71:369–396. [PubMed: 660156]
47. Sampath AP, Matthews HR, Cornwall MC, Fain GL. Bleached pigment produces a maintained decrease in outer segment Ca²⁺ in salamander rods. *J Gen Physiol* 1998;111:53–64. [PubMed: 9417134]
48. Saga T, Scheurer D, Adler R. Development and maintenance of outer segments by isolated chick embryo photoreceptor cells in culture. *Invest Ophthalmol Vis Sci* 1996;37:561–573. [PubMed: 8595956]
49. Kaplan MW, Iwata RT, Sterrett CB. Retinal detachment prevents normal assembly of disk membranes in vitro. *Invest Ophthalmol Vis Sci* 1990;31:1–8. [PubMed: 2298531]
50. Hale IL, Fisher SK, Matsumoto B. Effects of retinal detachment on rod disc membrane assembly in cultured frog retinas. *Invest Ophthalmol Vis Sci* 1991;32:2873–2881. [PubMed: 1833357]
51. McBee JK, Palczewski K, Baehr W, Pepperberg DR. Confronting complexity: the interlink of phototransduction and retinoid metabolism in the vertebrate retina. *Prog Retin Eye Res* 2001;20:469–529. [PubMed: 11390257]
52. Hattar S, Liao HW, Takao M, Berson DM, Yau KW. Melanopsin-containing retinal ganglion cells: architecture, projections, and intrinsic photosensitivity. *Science* 2002;295:1065–1070. [PubMed: 11834834]
53. Berson DM, Dunn FA, Takao M. Phototransduction by retinal ganglion cells that set the circadian clock. *Science* 2002;295:1070–1073. [PubMed: 11834835]
54. Gleason E, Mobbs P, Nuccitelli R, Wilson M. Development of functional calcium channels in cultured avian photoreceptors. *Vis Neurosci* 1992;8:315–327. [PubMed: 1314087]
55. Solessio E, Mani SS, Cuenca N, Engbretson GA, Barlow RB, Knox BE. Developmental regulation of calcium-dependent feedback in *Xenopus* rods. *J Gen Physiol* 2004;124:569–585. [PubMed: 15504902]
56. Schnetkamp PP. How does the retinal rod Na-Ca+K exchanger regulate cytosolic free Ca²⁺? *J Biol Chem* 1995;270:13231–13239. [PubMed: 7539424]

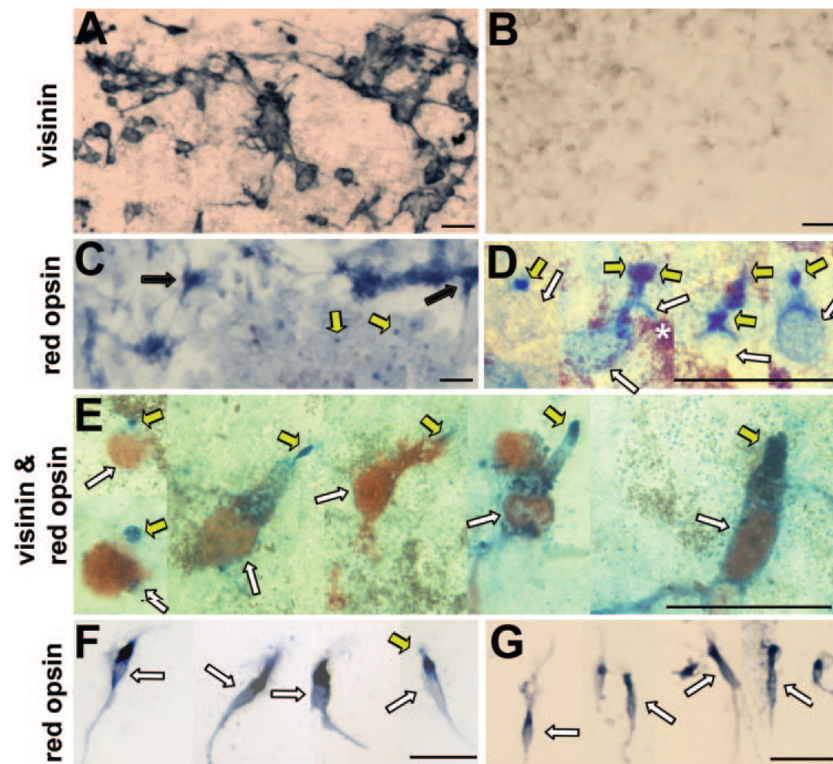


FIGURE 1. Subcellular localization of red opsin examined with immunostaining. (A, B) Anti-visinin immunostaining of primary RPE cell cultures infected with RCAS-neuroD (A) or RCAS-GFP (B). (C, D) Anti-red opsin immunostaining of primary RPE cell cultures infected with RCAS-neuroD. (E) double-staining with antibodies against visinin (*red*) and red opsin (*blue*). (F) Reprogrammed cells after reseeding onto a polyornithine-treated coverslip. (G) E17 retinal cell culture. *Black arrow*: cluster of cells with anti-red opsin immunostaining mostly in the cell body. *Yellow arrow*: cell's apex decorated by anti-red opsin immunostaining. *White arrow*: cell body. Scale bar, 20 μm .

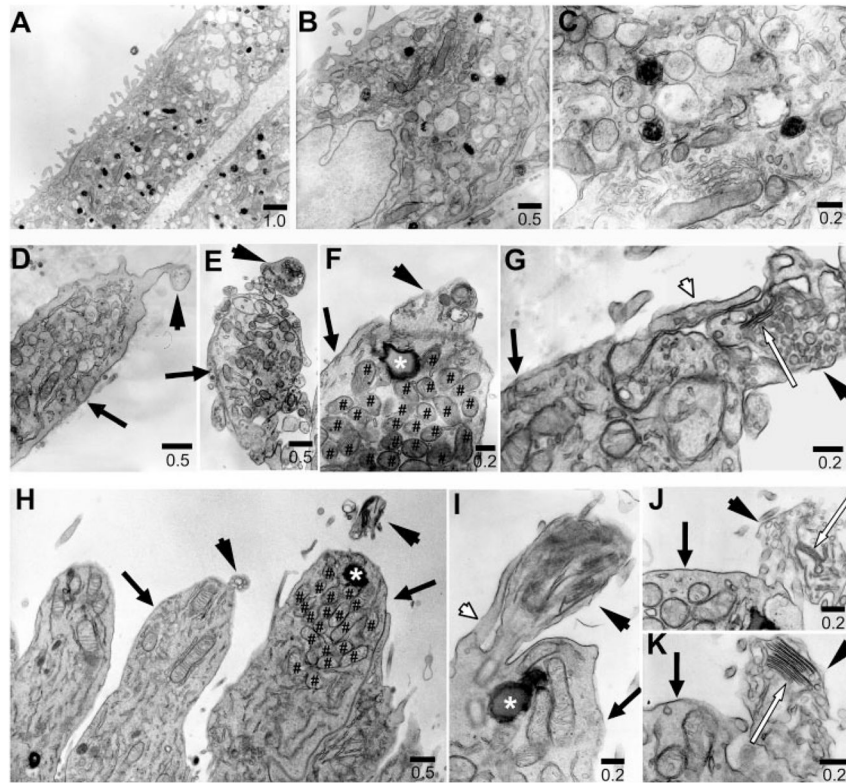


FIGURE 2. Ultrastructural features examined with electron micrography. (A–C) Cells in the control RPE cell culture. (D–G) Reprogrammed cells. (H–K) developing photoreceptors in E17 chick retina. *Arrow*, inner segment; *arrowhead*, rudimentary outer segment compartment; *white arrow*, discs; *white arrowhead*, calyx; *, lipid droplet; #, mitochondria. Scale bars are in micrometers.

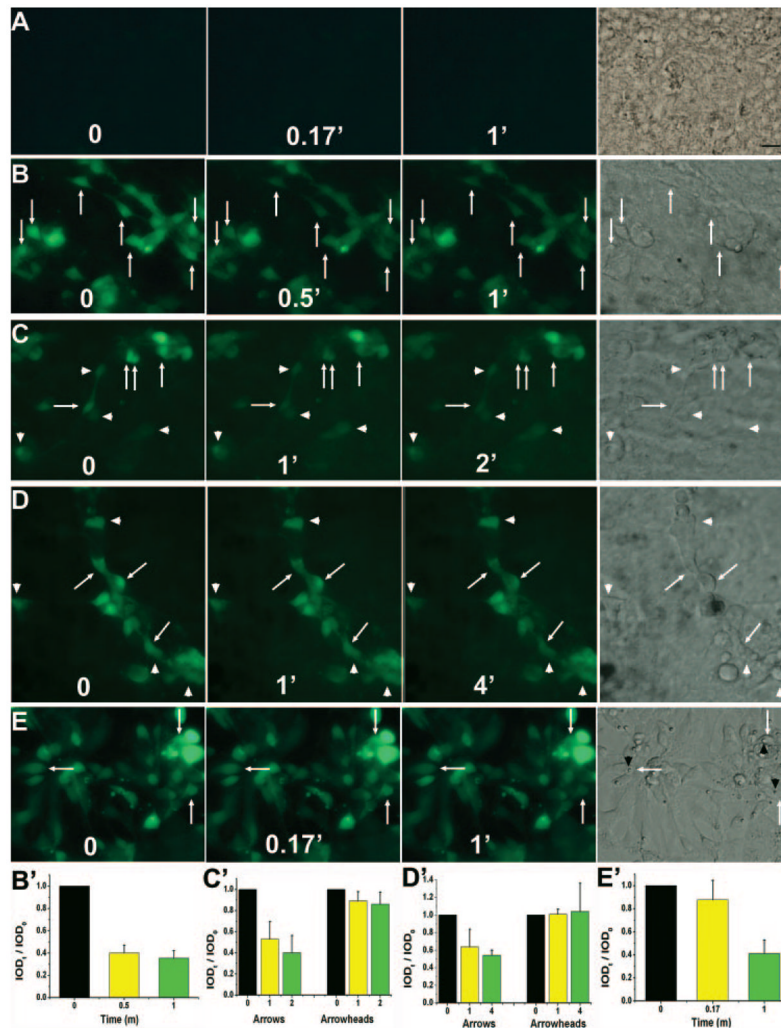
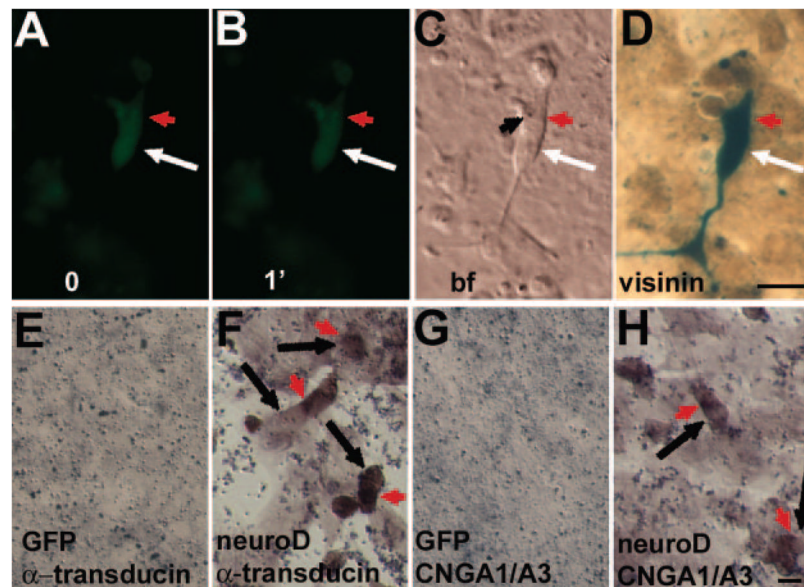


FIGURE 3.

Light response examined with Ca^{2+} imaging. (A) images before (0) and at different times (in minutes) of exposure to light of a control RPE cell culture infected with RCAS. A bright-field image is provided on the left. (B–D) Images of RPE cell cultures infected with RCAS-neuroD. (E) Images of E16 chick retinal cells after 3 days in culture. *Arrow*: a cell with noticeable reductions in fluorescence intensities; *arrowhead*, a cell lacking such reductions; *black arrowhead*, the lipid droplet. (B'–E') Calculated IOD ratios ($\text{IOD}_t/\text{IOD}_0$) shown as means and SDs of three to nine cells within the same image of (B–E), respectively. Scale bar, 10 μm .

**FIGURE 4.**

Detection for expression of genes involved in phototransduction. (A–D) Ca²⁺ imaging and postimaging immunostaining for visinin of an RPE cell culture infected with RCAS-neuroD. (A, B) Ca²⁺ imaging before (0) and after 1-minute (1') light exposure. (C) A bright-field image; (D) postimaging immunostaining for visinin; (E–H) in situ hybridization detection for expression of α -transducin (E, F) and CNGA1/A3 (G, H) in control RPE cell culture infected with RCAS-GFP and reprogrammed culture infected with RCAS-neuroD. *Arrow*: cell body; *red arrowhead*: inner-segment-like compartment; *black arrowhead*: lipid droplet. Scale bars, 10 μ m.

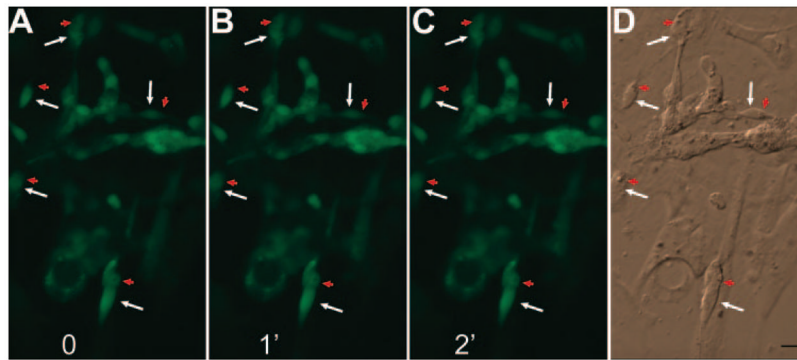
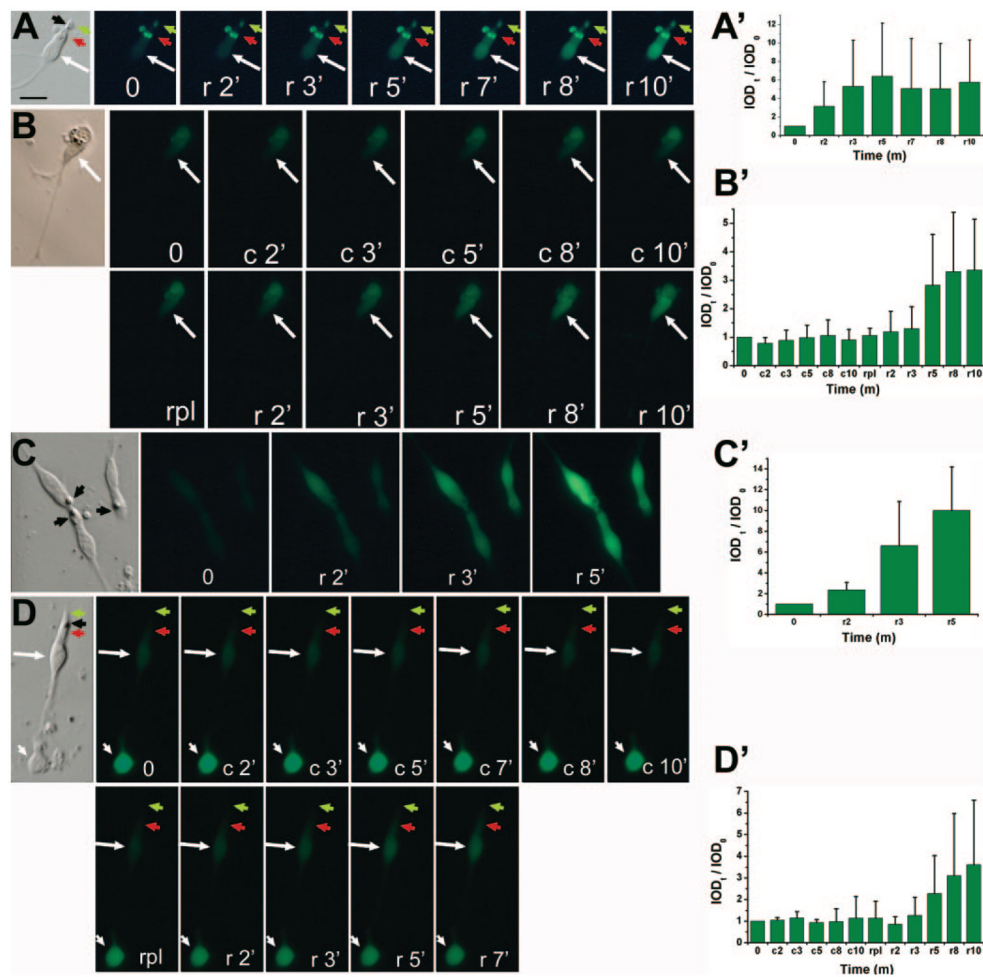


FIGURE 5. The effect of CNG channel blockers on light response examined with Ca^{2+} imaging. (A–C) Image before (0) and after exposure to light of 1 (1') and 2 (2') minutes of a RPE cell culture infected with RCAS-neuroD. (D) A bright-field image. *Arrow*: cell body; *red arrowhead*: inner-segment-like compartment. Scale bars, 10 μm .

**FIGURE 6.**

Response to 9-cis-retinal examined with Ca²⁺ imaging. (A) Images of a reprogrammed cell after bleaching (0) and at various time points (in minute) after administration of 9-cis-retinal (r). (B) Images of a reprogrammed cell after bleaching (0) and at various time points after sequential administration of vehicle control (c), replacement of M199 (rpl), and administration of 9-cis-retinal (r). (C) Images of photoreceptor cells (from E19 retina and cultured for 6 days) receiving the same treatment as in (A). (D) Images of E19 retinal cell culture (as in C) receiving the same treatment as in (B). Arrow: a cell showing increase in fluorescence intensities; white arrowhead: a cell lacking such an increase; black arrowhead: lipid droplet; red arrowhead: inner segment; green arrowhead: membranous expansion reminiscent of a rudimentary outer segment. The calculated IOD ratios (IOD_t/IOD₀) are shown as the means and SDs of three to nine cells from separate (different) images and marked as (A'-D') corresponding to experiments of (A-D), respectively. Scale bar, 10 μm.

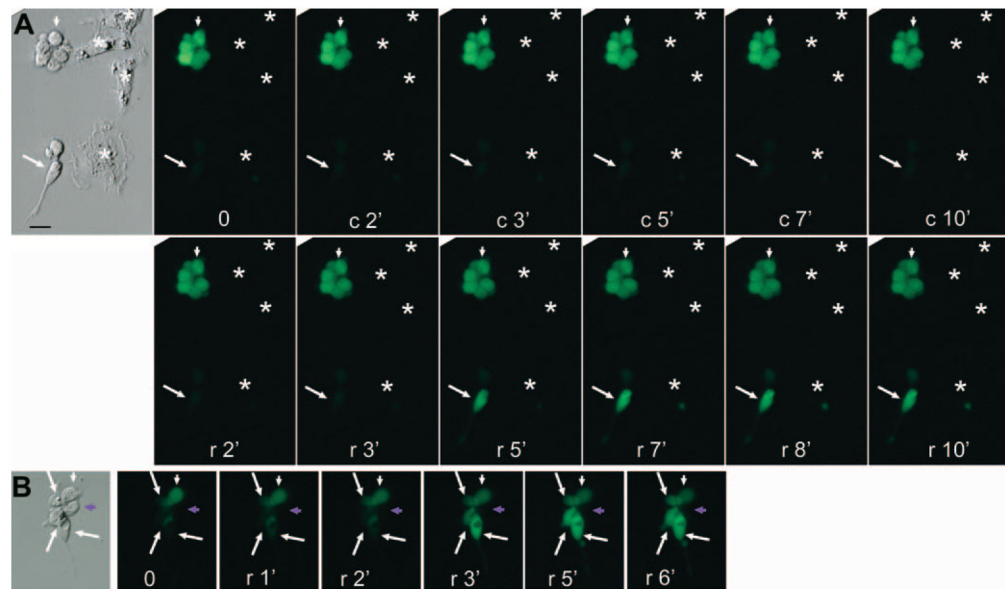


FIGURE 7.

Differential responses to 9-*cis*-retinal among cells with various morphologies examined with Ca^{2+} imaging. **(A)** Images of a responding photoreceptor-like cell (*arrow*) and a nonresponding round cell (*arrowhead*) and RPE cells (*****) in a reprogrammed cell culture after light bleaching (0), vehicle control (c), and 9-*cis*-retinal (r). **(B)** Images of responding photoreceptor-like cells (*arrows*) and nonresponding cells (*arrowheads*) in a cluster of cells in a reprogrammed cell culture after light bleaching (0) and 9-*cis*-retinal (r). *Purple arrowhead*: round cell that remained invisible to Ca^{2+} imaging. Scale bar, 10 μm .